

Aerodynamic Analysis of Bio-inspired Wing with Adaptive Aspect Ratio

Jini Raj R.^{1,*}, Praveen N.², Srikanth H.V.³, Mohammed Nijal⁴, Anil Umesh Bhat⁵

Abstract

The bio-inspired morphing wing is a futuristic concept in the aviation field that draws inspiration from birds and insects. Drawing inspiration from the exceptional flight capabilities of birds and insects, the goal is to develop a wing design that can adapt its aspect ratio, similar to nature. By incorporating the adaptive aspect ratio capabilities into the wing configuration, it becomes possible to optimize the wing's aerodynamic performance to adapt wide assortment of flight settings, including high-speed cruise and increased maneuverability. The wing aspect ratio is changed dynamically from a fully extended condition to a retracted condition through servo actuation. The aerodynamic characteristics of the retracted and fully extended conditions are analysed by Xfoil Low Reynolds number (XFLR5) simulations providing insights for performance optimization. The results show that by changing the aspect ratio to a fully extended condition, the lift-to-drag (L/D) ratio and lift coefficient (C_l) are increased and the drag coefficient (C_d) is reduced because of the reduction in induced drag. Similarly, at the retracted condition, the L/D ratio and C_l are reduced and the drag is increased. This capability can be adopted during high-speed turns and during instant landing, this wing is more efficient and can be adopted for all flight conditions thereby opening doors to new possibilities in the field of aerial vehicles and Unmanned Aerial Vehicles (UAV).

Keywords: Bio-inspired morphing, XFLR5, Aspect ratio, Aerial vehicles, UAV

INTRODUCTION

A bird's wing is made up of a movable skeleton, muscles and joints that are meticulous with soft overlapping feathers. By folding the outermost feathers, or primary flight feathers, a significant reduction in wing surface can be achieved. Almost all birds filled in the world have these adaptable

folding wings. The adaptable morphing wing can change shape without the need for wing surface slots or steps, reducing aerodynamic drag and being controlled automatically without pilot intervention. Like birds, these wings can spread or retract during various stages of flight, like perching, loitering, diving, or landing. Wing morphing is a technological advancement in the field of aviation that has the potential to adapt the wing shape during its flight. The name morphing originated from the word morphos word, which means change or transformation. Many researchers around the world worked on the bioinspired morphing concept. The morphing wing is the technological advancement of conventional aircraft and UAVs. A rational morphing wing can make the UAV with a better L/D ratio, adaptability and enhanced endurance [1]. The morphing concept is inspired by bird wings with key advantages such as Aerodynamic

*Author for Correspondence

Jini Raj R.

¹Assistant Professor, Aeronautical Department, Nitte Meenakshi Institute of Technology Bangalore, Karnataka, India

²Assistant Professor, Aeronautical Department, Nitte Meenakshi Institute of Technology Bangalore, Karnataka, India

³Associate Professor, Aeronautical Department, Nitte Meenakshi Institute of Technology Bangalore, Karnataka, India

^{4,5}Final Year Student, Aeronautical Department, Gopalan College of Engineering & Management Bangalore, Karnataka, India

Received Date: November 04, 2023

Accepted Date: January 02, 2024

Published Date: February 19, 2024

Citation: Jini Raj R., Praveen N., Srikanth H.V., Mohammed Nijal, Anil Umesh Bhat. Aerodynamic Analysis of Bio-inspired Wing with Adaptive Aspect Ratio. Journal of Polymer & Composites. 2023; 11(Special Issue 13): S143–S153.

efficiency, Flight envelope expansion, Enhanced maneuverability, Noise reduction, Design flexibility and Weight reduction [2]. This concept of nature-inspired wing morphing helps in solving human engineering challenges in the aviation industry.

Several attempts were made by researchers around the globe to improve the capability of Aircraft through bioinspired morphing. For example, Surface morphing is utilized by birds to energetically manipulate their posture and achieve aerodynamic excellence across a broad spectrum of flight velocities. Raj and Rose worked on a bioinspired morphing wing concept in the MQ-9 Reaper UAV. The Computational Fluid Dynamic transient analysis is carried out for the NACA 4412 airfoil that changes the airfoil shape dynamically and the benefits include improved L/D characteristics and delayed stall [3]. The main aspect of agile bird flight is in transforming the shape of the wing alternating between balanced and unbalanced gliding. The relevant research with morphing mechanism, airfoil configuration, material used and aerodynamic efficiency were discussed in this section.

Bioinspired morphing wing is categorized as follows: telescopic span morphing configuration, sweep morphing wing configuration, folded wing configuration, and Adaptable flexible wing [4, 5] Raj et.al developed a corrugated rib with a spine inspired by an eel fish that can morph the camber of the wing by adaptable flexible wing. The aerodynamic analysis suggests that the lift coefficient is increased during morphing. The ribs were 3D printed using polyactic acid plus (PLA+) material and the rib shape is NACA 4412 airfoil [6]. Ajanic et. al developed bio-inspired wings for drones with sweep morphing abilities that have been optimized for different flight regimes. By sweep morphing, the wings were retracted and extended for cruise and aggressive flight conditions [7]. Cheney et. al captured three different bird flying abilities during high-speed maneuvers and reported that it tends to bend the wing like a saddle shape at high-speed maneuvers [8]. Hui et. al investigated the aspect ratio adapting concept through a bioinspired morphing wing inspired from the pigeon. Interestingly, the wing offers an enhanced L/D ratio and reduced drag. The morphing is enabled through a pulley mechanism and the wing tip is made up of feathers just like birds [9]. Song et. al (2021) reviewed thoroughly the mechanism of birds's wings and the physics behind bird flight with both aerodynamic and structural analysis [10]. Harvey and Inman investigated the gull wing and found that the gull will adjust its shoulder and wing to do agility and high-speed maneuvers [11]. Yun et. al developed a retractive folding mechanism with sarrus linkage for a bio-inspired morphing wing UAV and found that the UAV can be fitted for sports and for different flight phases [12]. Matloff et. al reported that the feather arrangement of birds while extending their wings was because of the directional velcro mechanism and this aspect ratio adapting mechanism increases the aerodynamic efficiency of the wing during turbulence. conditions [13]. Retracted and extended morphing wings have their own superiority and extremities. When the wing is in an extended position it exhibits enhanced endurance and induced drag is also reduced. On the other hand, when the wing is retracted the aerodynamic performance decreases gradually but the maneuverability of the wing is enhanced [14, 15].

The swept wing is an adaptable design that helps in varying the sweep angle of the UAV to optimize aerodynamic efficiency. Conversely, when a UAV is about to make a dive in the water, the sweep angle is increased to tuck the wing closer to the fuselage, leading to a shorter wing span and contact area. This minimizes the impact of water entry and reduces drag during submersion but the hinge mechanism is more complex [16–18]. Normally, the wing can enable retraction through a mechanical linkage, gear assemblies, and torsion spring–pulley mechanism. To fit the wing for multiple mission phases of a collapsible aircraft, Wang et al. [19] developed a distinctive folding wing mechanism inspired by a beetle. Zhang et. al [20] developed a folding wing mechanism for a micro air vehicle (MAV). Ryu et. al. [21] coupled flapping and folding motion with a four-bar linkage mechanism.

Additionally, Luca et. al introduced morphing in small-winged drones that can retract its wing by sweeping them backwards to adapt their maneuvering capability. By inhibiting this ability, it can fly efficiently through obstacles and high wind resistance that cannot be optimally addressed by a single

aerodynamic profile [22]. Kilian et. al developed a prototype inspired by crow wings with bioinspired morphing capabilities, imitating real feather structures, and used an S1223 airfoil to provide smooth airfoil surfaces. The wingspan is retracted and extended through morphing and it shows aerodynamic performance, as confirmed by wind tunnel experiments [23]. Several bird species solve this problem by adapting the aspect ratio of their wings to adapt to the different aerodynamic requirements. This project aims to develop a retractable mechanism mimicking the Peregrine falcon bird and to study the aerodynamic behaviour of both wing configurations. During the descent and sudden dive phase, birds retract their wings to cut down the lift generated to drop down from a higher altitude to a lower altitude. This phenomenon is investigated in this aerodynamic analysis to evaluate the C_l and C_d behavior of the designed wing at both extended and retracted conditions. This ability enhances the UAVs to mimic birds and adapts its wing for different flight regimes.

METHODOLOGY

The methodology adapted in this work is illustrated in Figure 1. The morphing analysis starts with problem definition, geometry preparation, 2D analysis, 3D analysis, and evaluation of results and ends with the fabrication of the prototype.

DESIGN OF BIOINSPIRED WING

The bioinspired morphing wing configuration is inspired by Falcon Columbarius commonly named Falcon. The wing configuration of a Falcon bird changes its wing aspect ratio in two manners a fully extended shape and a retracted shape as displayed in Figure 2a and 2b.

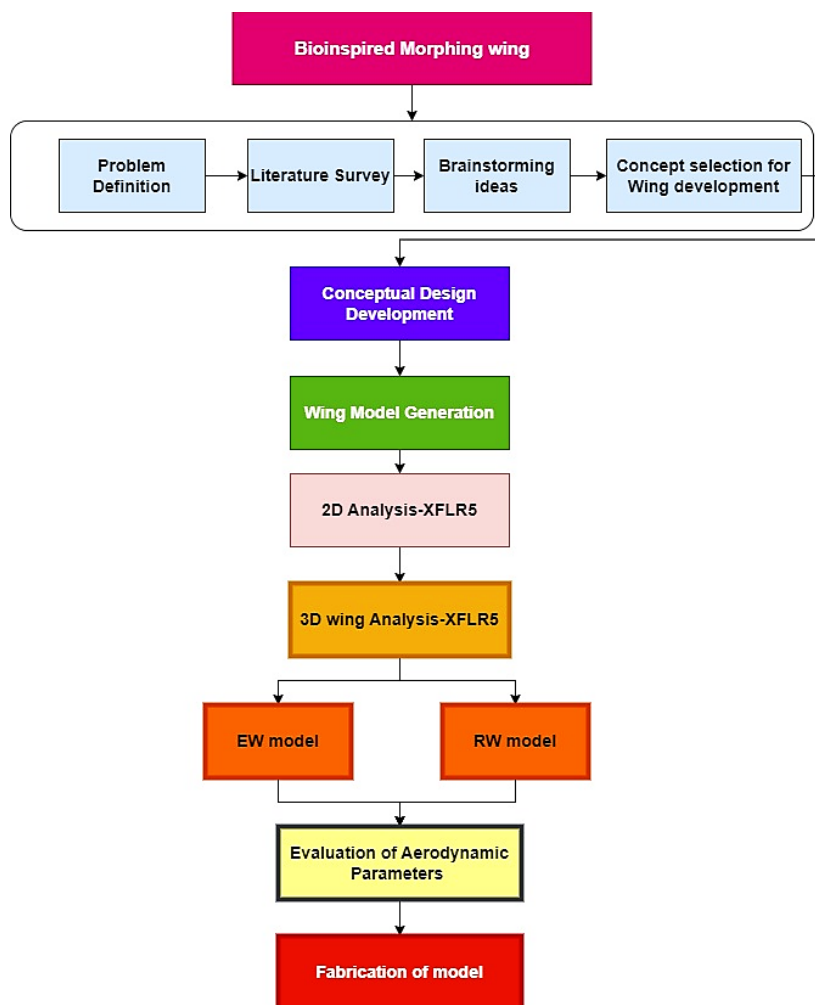


Figure 1. Methodology of Adaptive wing morphing.

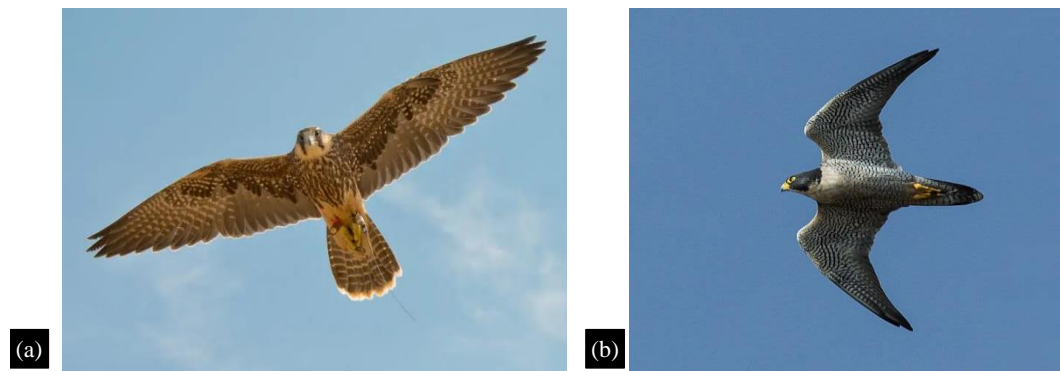


Figure 2. Morphed wing configuration of Falcon bird. (a) Fully Extended Wing (b) Retracted Wing.

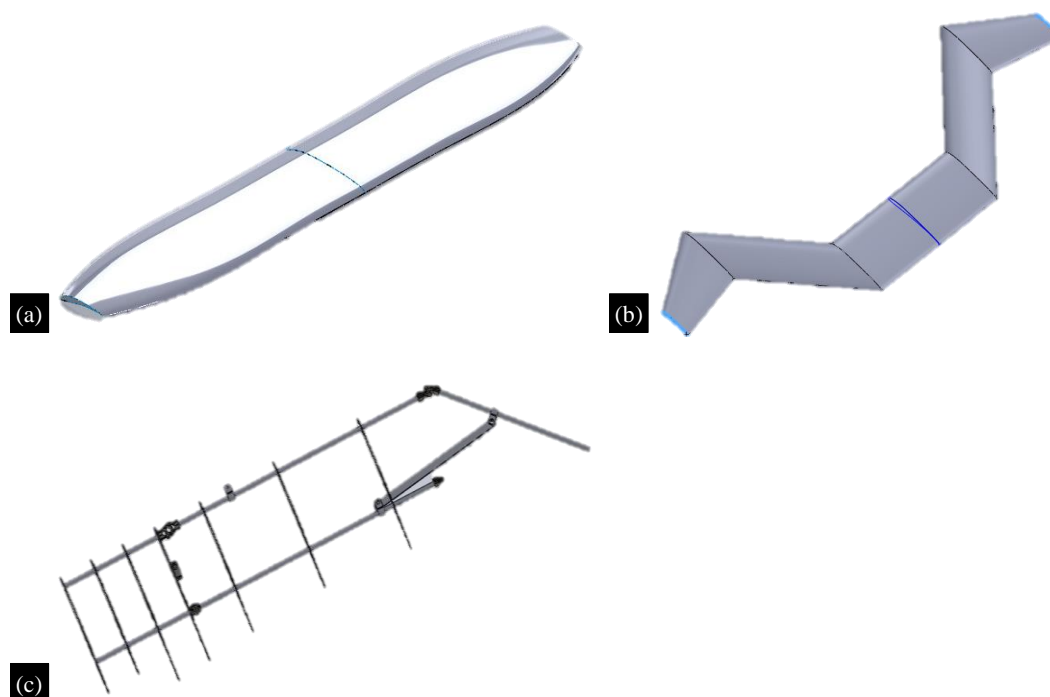


Figure 3. CAD model of morphed wing configuration. (a) Fully Extended Wing, (b) Retracted Wing, (c) CAD model of Morphing mechanism.

The CAD model is prepared by using the CATIA V5 tool for both the full extended wing and retracted wing configuration as presented in Figure 3. The length of the full extended wing is 0.7 m and the retracted wing is 0.55 m which is taken from the falcon wing. The airfoil used is S1223 and conventional NACA 4412 airfoil. S1223 airfoil is a high lift low Re number airfoil designed by Selig [24]. The C_{lmax} of the S1223 airfoil is high as compared to the conventional airfoil and it resembles the airfoil shape of a Falcon bird.

Birds change their wing aspect ratio by the internal muscles, bones and joints that enable the morphing as shown in Figure 4a and 4b [25]. The muscles are breast muscles (pectoralis and supracoracoideus) and the joints are wrist and elbow joints. Similarly, the morphed wing is designed with aluminium rods which act as a bone as seen in birds and hinges which act as joints the muscles that promote the aspect ratio changing motion are the servo, hinge and connecting rod (Figure 4c). The ribs are 3D printed with PLA material and the aluminium rods are about 5mm in diameter. The internal mechanism of the morphing wing has the capability of changing the aspect ratio from a fully extended condition to a retractive condition.

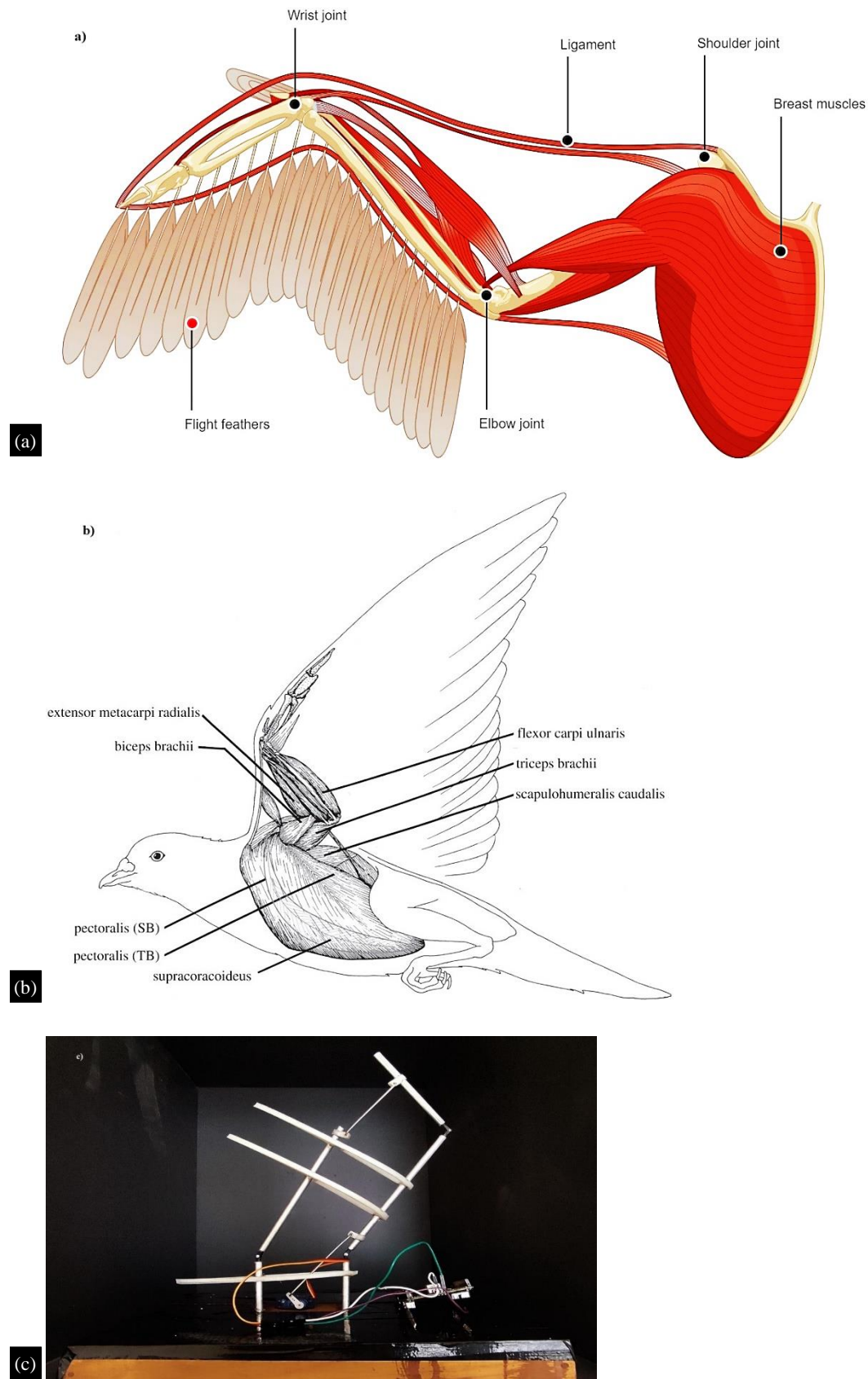


Figure 4. Bio-inspired Retractive Mechanism [25]. (a) Joints of birds promoting retractive motion, (b) Muscles providing retraction [25], (c) Bio-inspired morphing mechanism.

AERODYNAMIC ANALYSIS OF MORPHING WING

The aerodynamic analysis is carried out for two different morphing wing configurations i.e., retracted wing (RW) configuration and extended wing (EW) configuration. Initially, a low Reynolds number high lift airfoil S1223 and conventional thick airfoil NACA 4412 suitable for UAVs are taken for the analysis. The Reynolds number used for the analysis is 1.4×10^5 and the span length of EW and RW are 0.7m and 0.55m. The analysis is carried out for an angle of attack (AoA) range of about -15° to 15° . The simulation is done in the XFLR5 tool and the aerodynamic characteristics of the airfoil profile such as the lift coefficient (C_l) and drag coefficient (C_d) of both airfoils are analyzed.

Aerodynamic Coefficients of Airfoil Configuration

Figures 5a and 5b represent the C_l and C_d of both S1223 and NACA 4412 airfoil. The maximum lift coefficient C_{lmax} of S1223 and NACA 4412 are 2.135 and 1.322 respectively. At low Reynolds number (Re) S1223 shows significant performance but at high Re NACA 4412 is commercially used. Moreover, the stalling angle of NACA 4412 is high as compared to S1223. The C_d of S1223 is comparatively high compared with NACA 4412. Also, the maximum L/D ratio of NACA 4412 is 64 at 9° AoA and that of S1223 is 61 at 2° AoA as displayed in Figure 5c. This evidences that the selected airfoil for the bioinspired morphing strategy is virtuous to proceed with the analysis.

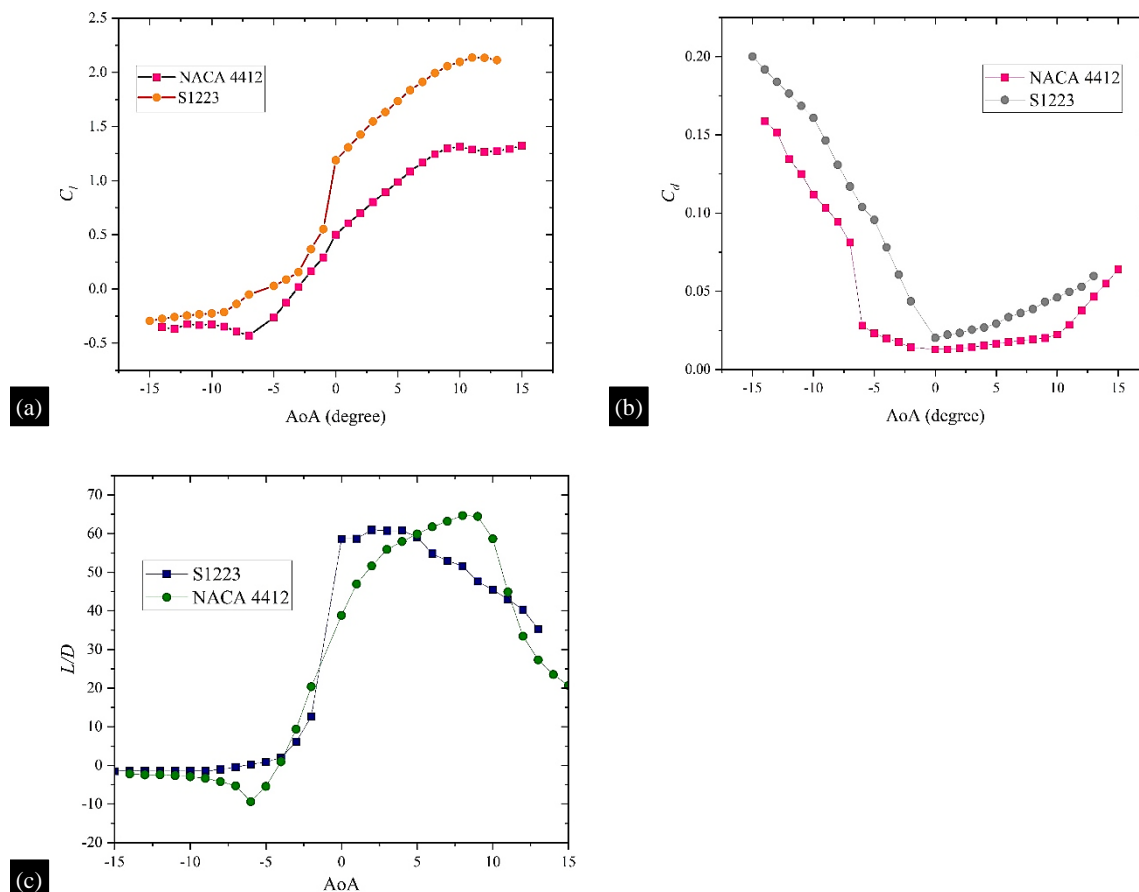


Figure 5. Aerodynamic coefficients vs AoA. (a) C_l vs AoA, (b) C_d vs AoA, (c) L/D ratio of airfoil configuration.

Pressure Coefficients (C_p) of Airfoil Configuration

The C_p of both NACA 4412 and S1223 airfoils are simulated through the XFLR5 tool and displayed in Figure 6. The C_p is computed for both airfoils from the low AoA range to the high AoA range. The low AoA range is scaled from 0° to 6° and the high AoA range is scaled above 6° . The C_p is plotted against x/c for both NACA 4412 and S1223 airfoil.

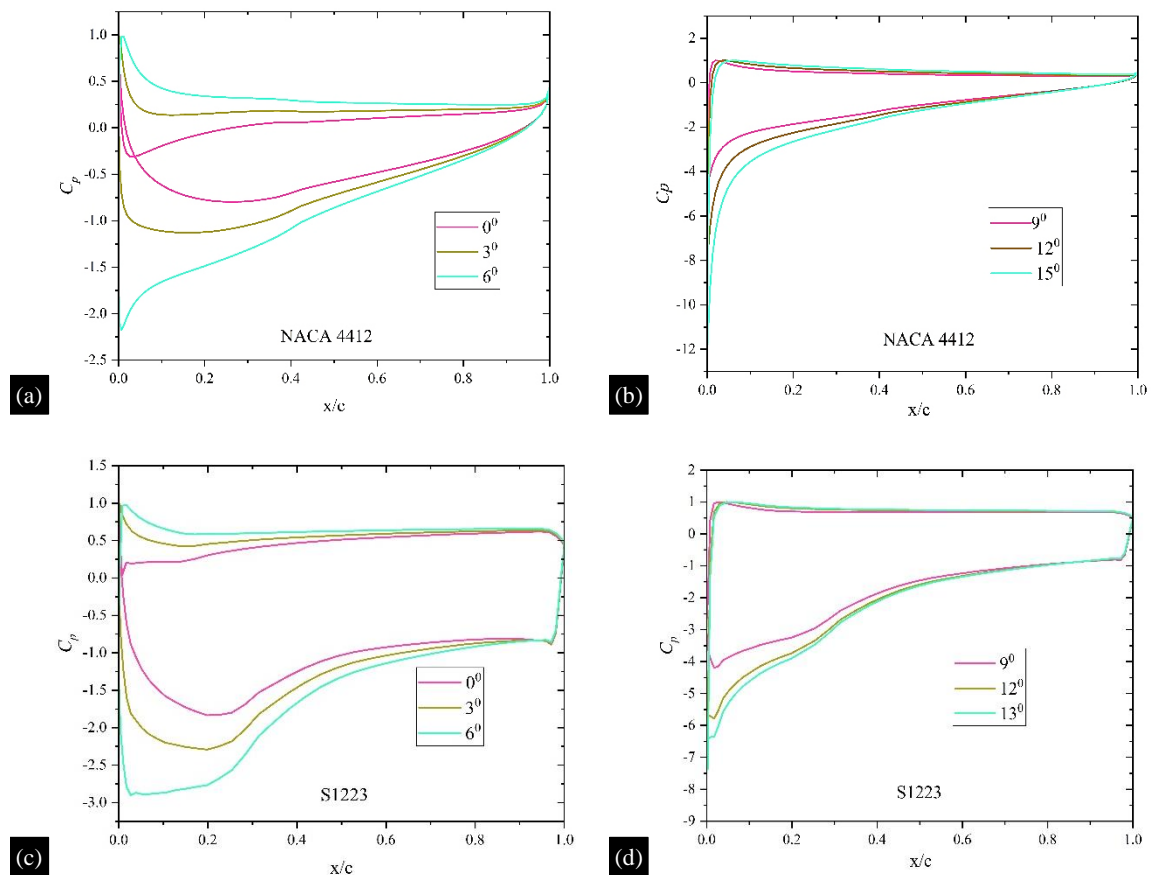


Figure 6. Pressure distributions around the 2D airfoil. (a) C_p low AoA NACA 4412 (d) C_p high AoA NACA 4412 (c) C_p low AoA S1223 (d) C_p high AoA S1223.

At low AoA, the C_p range of NACA 4412 is from -2.3 to 1.0 and at high AoA, the C_p value range increase from -11 to 1 as shown in Figure 6a and 6b. The pressure difference created because of the cross section shape is large enabling a maximum L/D ratio. Similarly, at low AoA, the C_p range of S1223 is from -3 to 1.0 and at high AoA, the C_p value range increases from -7 to 1 approx. as shown in Figures 6a and 6b.

In the S1223 airfoil, the camber of the airfoil is more compared to the conventional NACA 4412 airfoil. The trailing edge is cusped and that enhances the C_l even at low AoA but the airfoil stalls quickly. If this S1223 airfoil is implemented for the 3D rectangular wing, it will stall soon. Interestingly, Figure 6c and 6d showed that the cusped is responsible for the large gap in the C_p curve near the trailing edge. Even though the C_{lmax} of S1223 is high compared with the NACA 4412 model, the L/D ratio shows that NACA 4412 is superior to the S1223 airfoil

Aerodynamic Characteristics of EW and RW

The aerodynamic parameters like the lift distribution, downwash, induced drag and viscous drag are estimated to evaluate the performance of this adaptive aspect ratio wing. Both the EW and RW configuration is analyzed with the help of the XFR5 tool. The Aerodynamic characteristics of EW for a span length of 0.7 m at AoA 0° , 5° , 10° and 15° respectively are shown in Figure 7. The lift distribution of the adaptive wing is indicated with a vertical arrow (green colour) perpendicular to the surface of the wing. The arrow indicates that the lift distribution of the wing is more at the root region of the EW wing and near the wingtip the lift distribution is zero. As AoA increases the lift distribution is also increased as shown in Figure 7a–7d. The horizontal lines (yellow colour) emanating from the wing trailing edge portion show induced drag, which is more near the wingtip and less near the wing root as AoA increases.

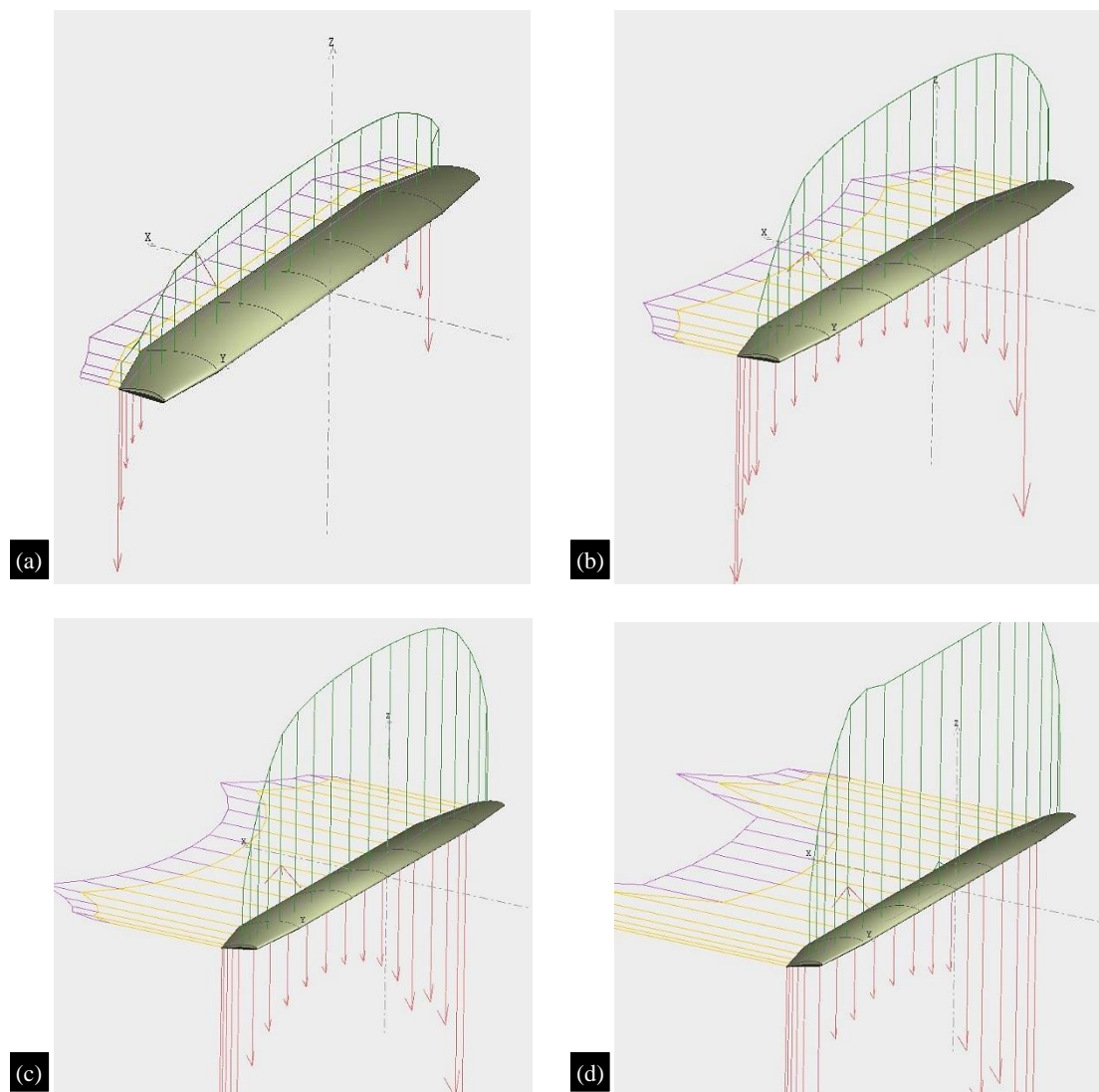


Figure 7. Aerodynamic characteristics of EW. (a) 0° AoA (b) 50° AoA (c) 100° AoA (d) 150° AoA.

The perpendicular line (red colour) acting in the downward direction is due to the downwash of the wing. It clearly states that as AoA increases from 0° to 15° AoA, the downwash is increasing substantially. Another set of horizontal lines (lavender colour) that extends after the induced drag lines are created due to the viscous drag on the wing profile. As AoA is increased, the viscous drag also arises shown in Figure 7d. At 15° AoA, the EW shows that the viscous drag formed due to the boundary layer separation is larger near the root region of the wing.

In contrast, the RW of span length 0.5m swept forward is analyzed at low Re and AoA range of 0° to 15° to determine its aerodynamic performance. The lift distribution of RW at low AoA shows that there is a considerable amount of reduction in the overall spanwise lift production during the glide phase (see Figure 8a and 8b). Figure 8c and 8d represent the lift distribution of RW at 10° and 15° AoA is reduced as compared with EW (see Figure 6c and 6d). This reduction in C_l paves the UAV to reduce its speed during maneuvers. The induced velocity is higher during this transition creating a downwash. The transition also indicates that the viscous drag is less compared to the EW configuration. This allows UAVs to do acrobatic maneuvers in extreme flight conditions.

The C_L and C_D of EW and RW with both airfoil configurations are displayed in Figure 9. Figure 9a shows that the NACA 4412 extended wing shows a 10% increase in lift compared with the retracted

wing after 5° AoA. However, the S1223 airfoil shows a 20% reduction in lift at low AoA, as the aerodynamic characteristic of this particular airfoil is good at low AoA (see Figure 9b). Similarly, the C_D of RW with NACA 4412 airfoil shows a 20% increase in drag at high AoA compared with the EW wing (see Figure 9c). But in the S1223 case, the EW shows an abrupt increase in C_D value at high AoA. The C_D of the RW is 10% higher than EW in all low AoA cases (see Figure 9d). Thus, it is evident that the RW aerodynamic characteristics change drastically and make it adaptable for circumstances like unexpected landing, high-speed maneuvers and acrobatic conditions.

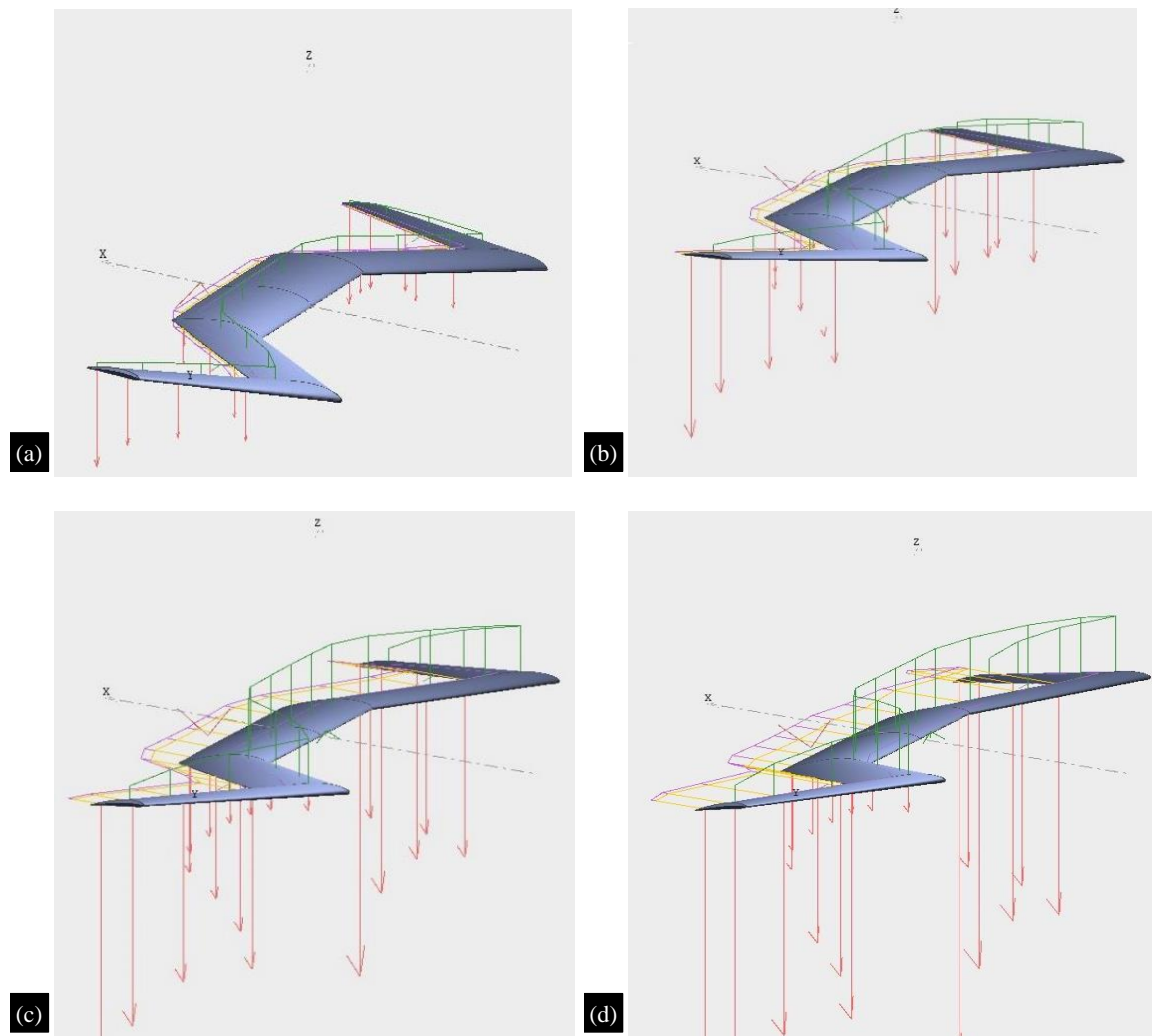
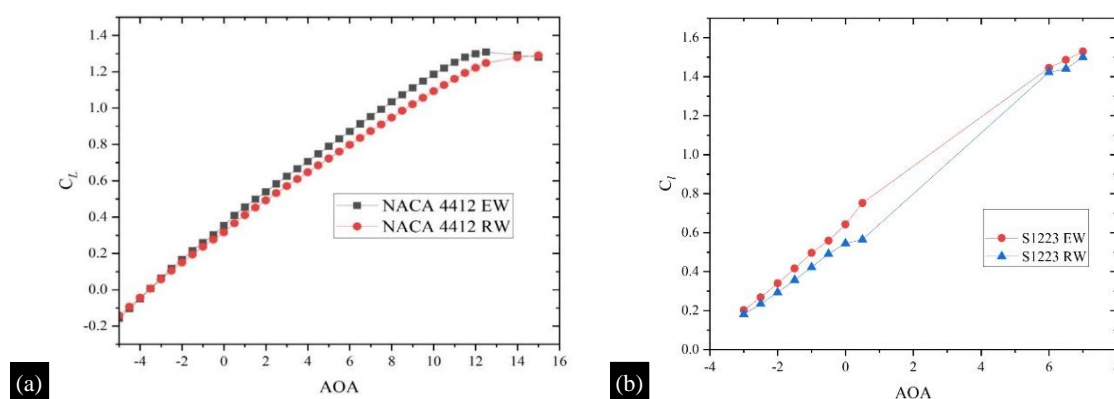


Figure 8. Aerodynamic features of RW (a) 0° AoA (b) 5° AoA (c) 10° AoA (d) 15° AoA.



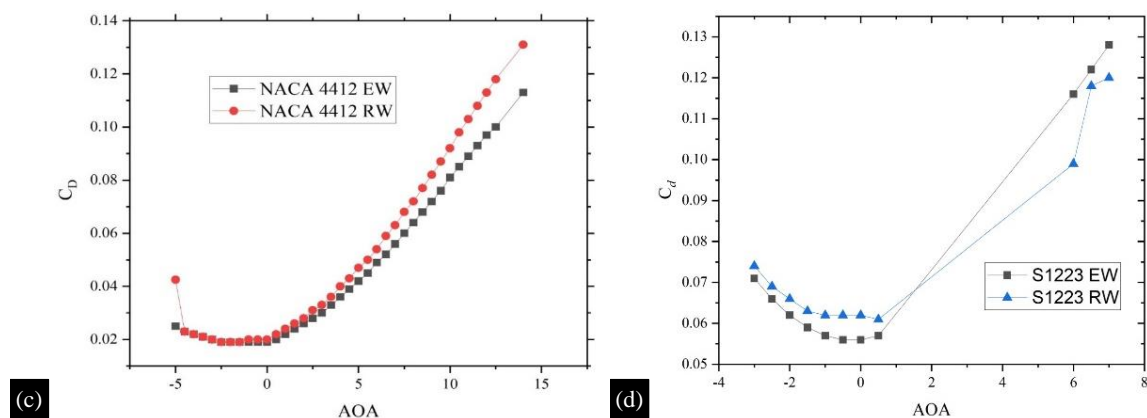


Figure 9. Aerodynamic coefficient of 3D wing (a) C_L of Wing with NACA 4412 airfoil (b) C_L of Wing with S1223 airfoil (c) C_D of Wing with NACA 4412 airfoil (d) C_D of Wing with S1223 airfoil

CONCLUSIONS

The bio-inspired wing with adaptive aspect ratio mechanism inspired by a falcon wing is developed to facilitate different aspect ratios during its flight. The internal components consist of hollow aluminium tubes, hinges and 3D-printed ribs. Also, 3D models were created to determine the aerodynamic coefficients of the wing at EW and RW conditions using the XFLR5 tool. The wing aspect ratio is changed dynamically from a fully extended condition to a retracted condition through servo actuation controlled by an Arduino board and a potentiometer. By incorporating the adaptive aspect ratio capabilities into the wing configuration, it becomes possible to optimize the wing's performance at different flight conditions that include high-speed cruise, instant landing and increased maneuverability. The results of the simulation show that by changing the aspect ratio to a fully extended condition, the L/D ratio and lift coefficient (C_L) are increased and the drag coefficient (C_D) is reduced from 10% to 20%. Similarly, at the retracted condition, the L/D ratio and C_L are reduced and the drag increases. This morphing wing technology enhances flight dynamics and stability of UAVs during high-speed turns and instant landings, offering potential advancements in various flight conditions.

REFERENCES

1. Barbarino S, Bilgen O, Ajaj R M, et al. A Review of Morphing Aircraft. *J. Intell. Mater. Syst. Struct.* 2011; 22; 823–877.
2. Klaassen van Oorschot B, Mistick E A, Tobalske B W. Aerodynamic consequences of wing morphing during emulated take-off and gliding in birds. *J. Exp. Biol.* 2016; 219; 3146–3154.
3. Jini Raj R, Bruce Ralphin Rose J. Flow physics and boundary layer optimization over a NACA airfoil by camber morphing at subsonic speeds. *Int. J. of Modern Phy. C*, 2023; 34; 06; 2350080, <https://doi.org/10.1142/S0129183123500808>.
4. Pendleton E W, Bessette D, Field P B, et al. Active Aeroelastic Wing Flight Research Program: Technical Program and Model Analytical Development. *J. Aircr.* 2000; 37; 554–561.
5. Gern F H, Inman, D J, Kapania R K. Computation of Actuation Power Requirements for Smart Wings with Morphing Airfoils. *AIAA J.* 2005; 43; 2481–2486.
6. Jini Raj R, Bruce Ralphin Rose J, & Vasudevan A. Analysis of Bio-inspired Fishbone Based Corrugated Rib for Adaptive Camber Morphing. *J Bionic Eng* 2023; 20; 1083–1102. <https://doi.org/10.1007/s42235-022-00326-6>.
7. Ajanic E, Feroskhan M, Mintchev S, et al. Bioinspired wing and tail morphing extends drone flight capabilities. *Science Robotics*, 2020; 5;47; eabc2897. doi:10.1126/scirobotics.abc2897.
8. Cheney J A, Stevenson J P J, Durston N E, et al. Raptor wing morphing with flight speed. *J. R. Soc. Interface* 2021; 18: 20210349. <https://doi.org/10.1098/rsif.2021.0349>.
9. Zhe H, Yang Z, Gang C. Aerodynamic performance investigation on a morphing unmanned aerial vehicle with bio-inspired discrete wing structures, *Aerospace Science and Technology*, 2019; Volume 95; 105419, ISSN 1270-9638, <https://doi.org/10.1016/j.ast.2019.105419>.

10. Song B, Lang X, Xue Dong et al. A review of the research status and progress on the aerodynamic mechanism of bird wings. *SCIENTIA SINICA Technologica*. 2021; 52. 10.1360/SST-2020-0515.
11. Christina Harvey and Daniel J I. Gull dynamic pitch stability is controlled by wing morphing, *Proceedings of the National Academy of Sciences*, 2022; 119; 37, e2204847119, 10.1073/pnas.2204847119.
12. Yun, Z, Feng, Y, Tang, X, et al. Analysis of Motion Characteristics of Bionic Morphing Wing Based on Sarrus Linkages. *Appl. Sci.* 2022; 12; 6023. <https://doi.org/10.3390/app12126023>
13. Matloff L Y, Chang E, Feo T J, et al. How flight feathers stick together to form a continuous morphing wing. *Science*. 2020; 367(6475):293-297. doi: 10.1126/science.aaz3358. PMID: 31949079.
14. Bae J S, Seigler T M, Inman D J. Aerodynamic and Static Aeroelastic Characteristics of a Variable-Span Morphing Wing. *J. Aircr.* 2005; 42; 528–534.
15. Samuel J B, and Pines D. Design and Testing of a Pneumatic Telescopic Wing for Unmanned Aerial Vehicles. *J. Aircr.* 2007; 44; 1088–1099.
16. Chakravarthy A, Grant D T, Lind R. Time-Varying Dynamics of a Micro Air Vehicle with Variable-Sweep Morphing. *J. Guid. Control. Dyn.* 2012; 35; 890–903.
17. Joo J J, Reich G W, and Westfall J T. Flexible Skin Development for Morphing Aircraft Applications via Topology Optimization. *J. Intell. Mater. Syst. Struct.* 2009; 20; 1969–1985.
18. Lindner D K, Bharti S, Frecker M, et al. Tendon actuated cellular mechanisms for morphing aircraft wing. *In Proceedings of the Modeling, Signal Processing, and Control for Smart Structures*, San Diego, 2007 March 19–21; CA, USA,.
19. Wang C, Ning Y, Chen L, et al. Design and Mechanical Analysis of Bionic Foldable Beetle Wings. *Appl. Bionics Biomech.* 2018; 1308465.
20. Zhang Z, Sun X, Du P, et al. Design of a hydraulically-driven bionic folding wing. *J. Mech. Behav. Biomed. Mater.* 2018; 82; 120–125.
21. Ryu S W, Lee J G, Kim H J. Design, Fabrication, and Analysis of Flapping and Folding Wing Mechanism for a Robotic Bird. *J. Bionic Eng.* 2020; 17; 229–240.
22. Di Luca M, Mintchev S, Heitz G et al. Bioinspired morphing wings for extended flight envelope and roll control of small drones. *Interface Focus*. 2017; 7: 20160092.
23. Lukas K, Farzeen S, Jing-Shan Z et al. Bioinspired morphing wings: mechanical design and wind tunnel experiments. *Bioinspir. Biomim.* 2022; 17 046019.
24. Selig M, & Guglielmo J. High-Lift Low Reynolds Number Airfoil Design. *J. Aircraft.* 1997; 34. 72-79. 10.2514/2.2137.
25. Dial K P, Activity patterns of the wing muscles of the pigeon (*Columba livia*) during different modes of flight. *J. Exp. Zool.* 1992; 262; 357–373. (doi:10.1002/jez. 1402620402)